Research Journal of Applied Sciences, Engineering and Technology 12(11): 1075-1081, 2016
DOI:10.19026/rjaset.12.2848
ISSN: 2040-7459; e-ISSN: 2040-7467

Submitted: September 12, 2015 Accepted: September 29, 2015 Published: June 05, 2016

Research Article

Mobility Performance Analysis of Mobile Robot Wheels

[1]Kutaiba Sabah Nimma, [2]Wajdi Sadik Aboud and [3]Sabah Nimma Faraj
[1]Department of Electrical and Electronic, Faculty of Engineering and Built Environment, Universiti Kebangsaan Malaysia, Malaysia
[2]Department of Prosthetics and Orthotics Engineering, Faculty of Engineering, University of AL-Nahrain,
[3]Department of Machinery and Equipment, Institute of Technology Baghdad, University of Middle Technical, Iraq

Abstract: Robotics is an interesting and rapidly developing field with many applications that extend from robot manipulators to mobile robots. This study focus on analysis a variety of mobile robot wheels based on their sizes, shapes, types of motion and properties. One of the most important parts of a mobile robot is the wheel. The use of wheels is the most well-known method of providing mobility to robots and propelling many different-sized robots and automatic platforms. Wheels can be any size-from fractions of an inch to 12 inches. Robots can have any number of wheels, with most mobile robots having three or four wheels. However, only a few studies have examined the dynamics of mobile robot wheels, as well as the time constant of the motor of mobile robot wheels. The dynamics of the mobile robot is examined and the time constant of two motors, which affects the direction of mobile robot motion, is controlled in this research. The results demonstrate that the mobile robot moves successfully from one location to another with a variety of speeds, directions and load on wheel's motors.

Keywords: AGV, dynamics, kinematics, mobile robot, robot, wheels

INTRODUCTION

Automatic Guided Vehicles (AGVs) have been found since the 1950s. AGVs are considered one of the driverless industrial trucks, which are normally powered by electric motors and batteries. AGVs have different sizes from carrying small loads of a few kg to loads of over 100 tons (Le-Anh and De Koster, 2006; Vis, 2006). The environments of working might be also change from offices with carpeted floors to harbor dockside spots. Modern AGVs are computer-controlled vehicles and use a wire guide (signal on a buried wire) combined with an onboard microprocessor or other control devices (Ronzoni *et al*., 2011). AGVs can be programmed to load, unload, accelerate, decelerate, stop, start and block and select travel paths-all without human intervention. The primary AGVs were built as tuggers and towing trailers or shaped as platform vehicles, known as mobile robots (Ronzoni *et al*., 2011). A mobile robot is an automatic machine that has capability of locomotion (i.e., the ability to travel around in the environment) and is not fixed to one physical place. The technical successes we have seen in robotics competitions over the years are finding their way into practical applications and one such application is the wheeled mobile robot (Choudhury, 2005; A˚ström and Kumar, 2014). A wheeled mobile robot is one type of a wheeled vehicle that is able to autonomous motion (i.e., without human interfere), due to it is supplied with actuators driven through an embarked computer (Fukao *et al*., 2000). Wheeled mobile robots are currently the focus of increasing attention in the scientific community and in many industries. Their potential applications in the field of service robotics and the development of microprocessors have made these systems easier to implement (Fukao *et al*., 2000; Papadopoulos and Poulakakis, 2000). Wheeled mobile robots are also considered more versatile than AGVs. Thus, wheeled mobile robots can be used in a wide range of applications, such as in hospitals, factories and other dangerous places.

In fact, wheeled mobile robots have been utilized to solve many mobility problems in recent years and are being developed for a range of mobility applications, including the simple control laws, based on tangential linearization or heuristic methods (Micaelli *et al*., 1989; Durieu *et al*., 1989; Sharma and Martin, 2009; Singh and Shin, 1989). Many general controllers have been proposed based nonlinear control theory (Kanayama *et al*., 1991; Morin and Samson, 2008; Sampei *et al*., 1991; Samson, 1992; Zhang *et al*., 2013), the trajectory tracking issue for robots that move on flat ground

Corresponding Author: Kutaiba Sabah Nimma, Department of Electrical and Electronic, Faculty of Engineering and Built Environment, Universiti Kebangsaan Malaysia, Malaysia

without skidding based on parameterization (Samson, 1992) and the relative path-to-vehicle distance for unicycle-type mobile robots and two-steering-wheel mobile robots (Samson and Micaelli, 1992). The focus of this study is to demonstrating the mobile robots ability to move through the operational space freely from one place to another without any constraints, such as friction, speed and direction of the robot wheels. Time constant of motors and mobile robot dynamicity are controlled and examined which represent the essential aspects of mobile robots.

MATERIALS AND METHODS

Types of wheels in mobile robots: The basic robot design, which has three essential parts (sensing block, control block and motor block) is presented in a block diagram shown in Fig. 1. The sensing block provides information from the environment, which surrounds the robot. The controller block generates control responses based on reaction type from the sensors. Finally, the motor block drives the motors of the wheels in different directions based on orders coming from the controller (Sampei *et al*., 1991; Samson and Micaelli, 1992).

Wheel is the basic part of the mobile robot, which is responsible for the way it moves. The two basic idealized wheels are the conventional wheels and the Swedish wheels (Papadopoulos and Poulakakis, 2000). The Swedish wheels are further classified into three types, namely, fixed wheel, steering wheel and caster wheel. For each type of Swedish wheel, we assume that the meeting points between the wheel and the ground is reduced to a single point of the plane, which indicates that only a single element of the velocity of the meeting point of the wheel with the ground must be zero along the movement of the wheel. The direction of this zero element of velocity is a priori arbitrary, but is fixed with regarding to the orientation of the wheel. Meanwhile, the conventional wheel contact between the wheel and the ground must satisfy the conditions of pure rolling and non-slipping along the wheel's movement. These conditions require that the velocity of the meeting point be equal to zero and that the two components, which are parallel to the plane of the wheel and orthogonal to the plane of velocity, should also be equal to zero.

Conventional wheels: Conventional wheels are further classified into three types, namely, fixed wheel, steering wheel and caster wheel.

A fixed wheel is shown in Fig. 2 and a streering wheel is shown in Fig. 3. In the figures, "A" denotes the middle of the fixed wheel, which is a constant point on the cart. Point A in the frame is defined using polar coordinates, namely, l and α.

The location of the wheel is characterized by four constants, namely, α, β, l and r. The motion of the wheel is characterized by a time-varying angle $\vartheta(t)$, β is a constant angle representing the orientation of the plane of the wheel with respect to l, r is the radius of the wheel

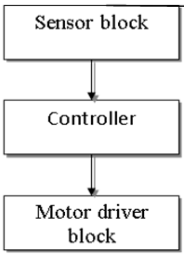

Fig. 1: Simplified block diagram of a mobile robot

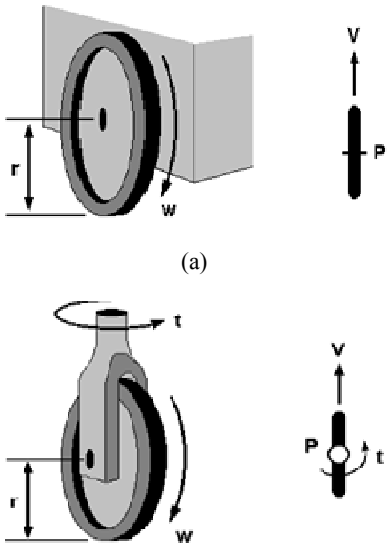

Fig. 2: Fixed wheel and wheel with direction

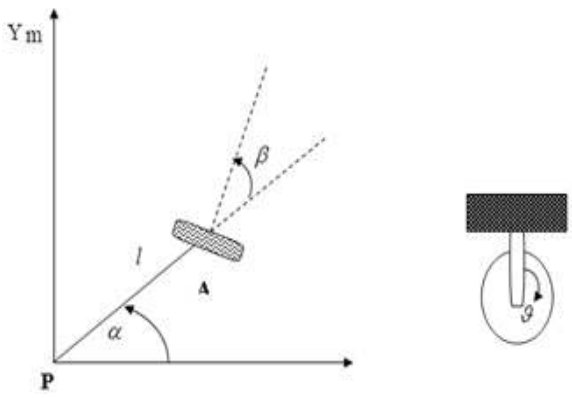

Fig. 3: Steering wheel

and $\vartheta(t)$ is the rotation angle of the wheel about its (horizontal) axle. This description of the velocity of the meeting point is governed through the following constraints:

$$\begin{matrix} -\sin(\alpha+\beta) & \cos(\alpha+\beta) & 1 & \cos\beta] \\ R(\varphi)\,\dot{\epsilon} + r\dot{\vartheta} = 0 \end{matrix} \quad (1)$$

$$\cos(\alpha+\beta) \quad \sin(\alpha+\beta) \quad 1 \quad \sin\beta]\, R(\varphi)\dot{\epsilon} = 0 \quad (2)$$

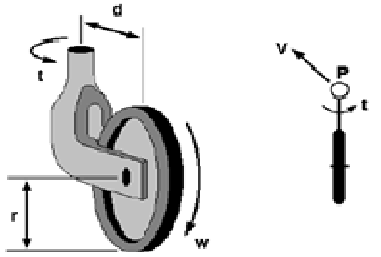

Fig. 4: Caster wheel

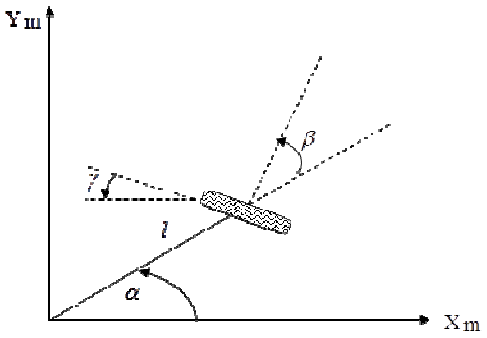

Fig. 5: Swedish wheel

$$\text{where } R(\varphi) = \begin{pmatrix} \cos\varphi & \sin\varphi & 0 \\ -\sin\varphi & \cos\varphi & 0 \\ 0 & 0 & 1 \end{pmatrix}, \dot{\epsilon} = \begin{pmatrix} \dot{X} \\ \dot{Y} \\ \dot{\varphi} \end{pmatrix}$$

Equations (1) and (2) are derived parallel to the wheel plane constraint and orthogonal to the wheel plane constraint, respectively. In addition, $R(\varphi)$ is the robot posture and orientation matrix.

For the steering wheel, the wheel plane motion with respect to the cart involves rotation about the vertical axle passing through the middle of the wheel (Fig. 3). The description is the same as that for the fixed wheel, except that the angle β is not constant but time-varying. Here, the position of the wheel is characterized by three constants, namely, l, α and r, relative to the motion of these constants with respect to the cart by two time-varying angles, namely, $\vartheta(t)$ and $\beta(t)$. The constant has the same form as that previously shown in Eq. (1) and (2).

The caster wheel is an orientable wheel with respect to the cart; however, the turning of the wheel plane is about the vertical axle, which does not pass over the middle of the wheel (Fig. 4):

$$\begin{matrix} -\sin(\alpha+\beta) & \cos(\alpha+\beta) & 1\cos\beta] \\ R(\varphi)\,\dot{\epsilon} + r\dot{\vartheta} = 0 \end{matrix} \quad (3)$$

$$\begin{matrix} \cos(\alpha+\beta) & \sin(a+\beta) & d+1\sin\beta] \\ R(\varphi)\,\dot{\epsilon} + d\dot{\beta} = 0 \end{matrix} \quad (4)$$

Swedish wheels: The location of the Swedish wheel with regard to the cart is similar to the position of the fixed wheel described in three constant parameters (β, α and l), as shown in Fig. 5. An extra parameter is needed to characterize the direction of the zero component of the velocity of the motion constraint, with regard to the wheel plane. This is governed by the following expression:

$$\begin{matrix} -\sin(a+\beta+\gamma) & \cos(a+\beta+\gamma) \\ 1\cos(\beta+\gamma) & R(\varphi)\dot{\epsilon} + r\cos\gamma\,\vartheta = \end{matrix} \quad (5)$$

MODELING OF THE TYPES OF MOTION DISPLAYED BY MOBILE ROBOTS

In this part, we demonstrate in detail the types of motion diplsyed by mobile robots: kinetic motion and dynamic motion.

Kinetic motion: Mobile robots have relatively simple mathematical models to describe their instantaneous motion capabilities compared with other robots. Kinematics point to the development of a mechanical system in the position and velocity, regardless to its mass and inertia. In this section, we analyze the kinematics of a 2-DOF differential drive vehicle (Fig. 6). The aim of the analysis is to show the relationship between all known or measurable locations and speeds and all quantities, which are measured by kinematics (Sharef *et al*., 2010).

Figure 7 illustrates the initial coordinate frame for a mobile robot, which are represented by X_0 and Y_0. The angle between the velocity vector and the initial X-axis is denoted by φ. The velocity trajectory of the robot center of mass is V_G, which is vertical to the wheel axis. The X and Y components are expressed as follows:

$$\dot{X}_G = V_G \cos(\varphi) \quad (6)$$

$$\dot{Y}_G = V_G \sin(\varphi) \quad (7)$$

where, V is the absolute velocity and ϑ is the angular velocity:

$$V_G = \frac{\dot{\vartheta}_L r + \dot{\vartheta}_R r}{2} = \frac{r}{2}\left(\dot{\vartheta}_L + \dot{\vartheta}_R\right) \quad (8)$$

The rotational velocity is calculated as follows:

$$\dot{\varphi} = \frac{V_R - V_L}{b} = \frac{r}{b}\left(\dot{\vartheta}_R - \dot{\vartheta}_L\right) \quad (9)$$

Rewriting Eq. (8) and (9), the angular velocities for the left and right wheels are derived as follows:

$$\dot{\vartheta}_L = V_G + \frac{b}{2}\dot{\varphi} \quad (10)$$

$$\dot{\vartheta}_R = V_G - \frac{b}{2}\dot{\varphi} \quad (11)$$

Differential kinematics is necessary for Point FP on the mobile platform to construct viable system trajectories. This point might be the base of a robotic

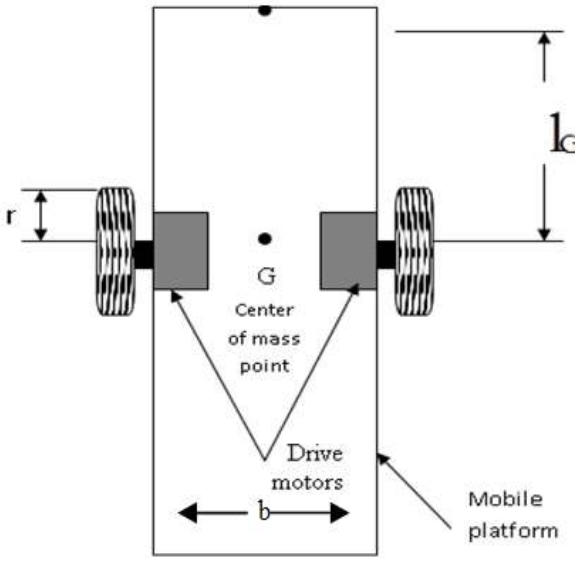

Fig. 6: Differential drive mobile robot

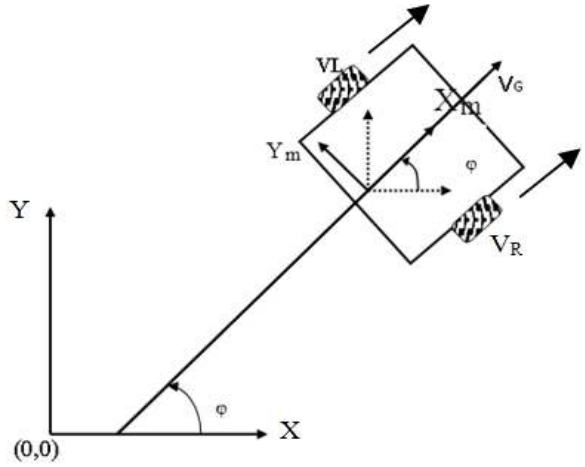

Fig. 7: Initial coordinate frame for a mobile robot

arm or a camera. Simple analysis shows that differential kinematics can be expressed as follows (2):

$$\begin{pmatrix} \dot{X}FP \\ \dot{Y}FP \\ \dot{\varphi} \end{pmatrix} = \begin{pmatrix} \frac{r}{2}\cos(\varphi) + \frac{l_G\, r\sin(\varphi)}{b} & \frac{r}{2}\cos(\varphi) - \frac{l_G\, r\sin(\varphi)}{b} \\ \frac{r}{2}\sin(\varphi) - \frac{l_G\, r\cos(\varphi)}{b} & \frac{r}{2}\sin(\varphi) + \frac{l_G\, r\cos(\varphi)}{b} \\ -\frac{r}{b} & \frac{r}{b} \end{pmatrix} \begin{pmatrix} \dot{\vartheta}L \\ \dot{\vartheta}R \end{pmatrix} \quad (12)$$

Dynamic motion: The dynamic motion of a mobile robot is represented by the relationship among force, torque and acceleration. The second part of the modeling of the robot's wheels (i.e., derivation) is divided into two

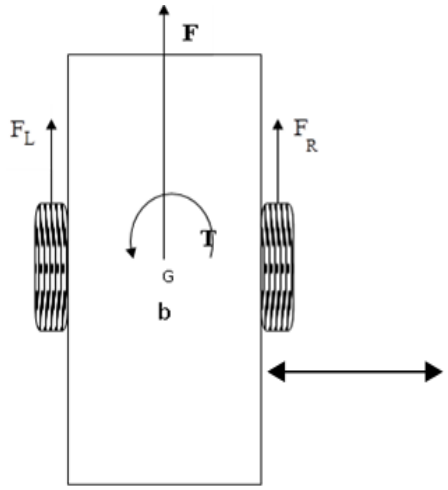

Fig. 8: Force model for a mobile robot

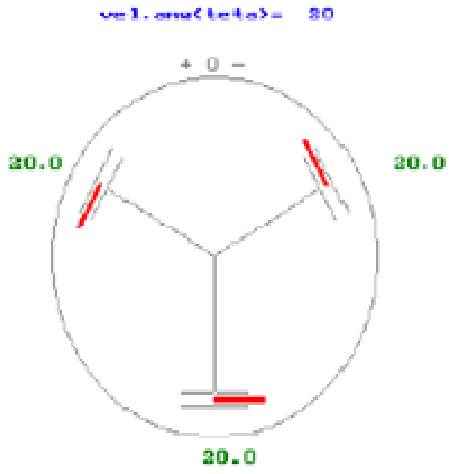

Fig. 9: Graphical representation of motor contributions for a positive angular velocity

types of wheel motion. First, we consider the translation or linear motion of the wheels; second, we consider the rotational motion of the wheels. For the differential drive mobile robot represented in Fig. 8, F is the force applying on the robot center of mass, T is the torque applying about the center of mass, F_R is the force exerted on the mobile robot by the right wheel, F_L is the force exerted on the robot by the left wheel and b is the distance between the two wheels.

The relationship between the speed of the mobile robot and wheel force is expressed as follows:

$$\begin{pmatrix} \dot{V} \\ \dot{\omega} \end{pmatrix} = \begin{pmatrix} \frac{1}{m} & \frac{1}{m} \\ \frac{b}{J} & -\frac{b}{J} \\ mr & mr \end{pmatrix} \begin{pmatrix} FR \\ FL \end{pmatrix} \quad (13)$$

Angular movement: For angular movement, accurate wheel alignment and pure rotation over its center must be assumed. Angular movement can be accomplished

by driving all wheels in the same orientation and at the same velocity. The angular velocity of rotation is the linear peripheral velocity of the wheels divided by the radius of the robot. Figure 9 shows the motor contributions for a positive angular velocity. As can be seen, the positive values cause the robot to move to the left, while the negative values cause the robot to move to the right direction.

EXPERIMENTAL SETUP AND DISCUSSION

In this study, the apparatus used in the experiment included a power supply, servo motor, potentiometer, oscilloscope, load and voltmeter (Fig. 10 and 11). The dead zone used in this study was 3.79.

Mobile robot wheel mobility was tested under several conditions and parameters established on the aforementioned devices. We analyzed the operation of mobile robot wheels at different voltages (4, 6 and 8 V) under varied scenarios. In the first scenario, the servo motor worked smoothly without any restrictions (load). In the second scenario, the servo motor was exposed to loads under different voltages (4, 6 and 8 V).

Without load: In this section, we evaluate the performances of mobile robot wheels when the servo motor operated without any load under different voltages (4, 6 and 8 V) at varied settling times (1, 2.5 and 3 Ts). These are all presented in Table 1.

We tested the robot wheels without any load under different voltages. When the applied voltage is 4 V, the signal is low, stabilized very fast with a settling time of 1 Ts and continued to stabilize with a final value of 1 (Fig. 12).

Meanwhile, when we applied 6 V to the motor with a settling time of 2.5 Ts, the signal became higher than the 4 V signal with a final value of 3.6 (Fig. 13).

However, when we applied 8 V to the motor with a settling time of 3 Ts, the signal became higher than the 4 and 6 V signals with a final value of 4 (Fig. 14).

With load: In this section, we evaluate the performances of mobile robot wheels affected by different voltages (4, 6 and 8 V) at varied settling times under two load values of 5 and 10.

With load = 5: The robot wheels were tested under a load value of 5 at different voltages (4, 6 and 8 V) and varied settling times (Table 2).

The signal in the oscilloscope is stable during the initial stage of the experiment. Then it increased steadily and became stable again with a final value of 0.32 at a voltage of 4 V and settling time of 1.4 Ts (Fig. 15).

Meanwhile, when we applied 6 V with a settling time of 1 Ts, the signal stabilized and increased significantly with a final value of 0.6 (Fig. 16).

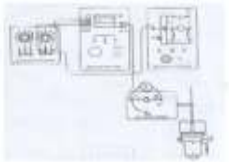

Fig. 10: Block diagram of the apparatus

Fig. 11: Apparatus used in the experiment

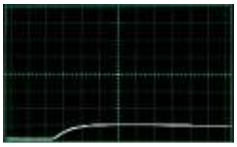

Fig. 12: Wheel performance simulation at 4 V and 1 Ts

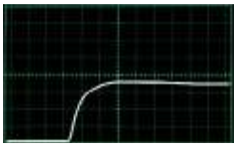

Fig. 13: Wheel performance simulation at 6 V and 2.5 Ts

Fig. 14: Wheel performance simulation with 8 V and 3 Ts

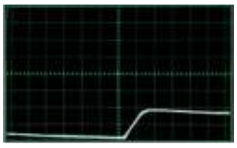

Fig. 15: Wheel performance simulation at 4 V and 1.4 Ts

Table 1: Experimental parameters without load

			Scales	
Voltage	Settling time (Ts)	Final value	V	H
4	1	1	1	0.5
6	2.5	3.6	0.5	0.5
8	3	4	1	0.5

Table 2: Experimental parameters under a load value of 5

				Scales	
Load	Voltage	Settling time (Ts)	Final value	V	H
5	4	1	0.32	1	0.5
	6	2.5	0.6	0.5	0.5
	8	3	0	1	0.5

Fig. 16: Wheel performance simulation at 6 V and 1 Ts

Fig. 17: Wheel performance simulation at 8 V and 1 Ts

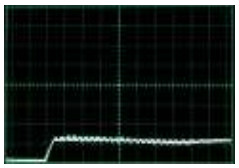

Fig. 18: Wheel performance simulation at 4 V and 0.25 Ts

Fig. 19: Wheel performance simulation at 6 V and 0.53 Ts

Fig. 20: Wheel performance simulation at 8 V and 1.5 Ts

Table 3: Experimental parameters under a load value of 10

				Scales	
Load	Voltage	Settling time (Ts)	Final value	V	H
10	4	1	0.1	1	0.5
	6	2.5	0.24	0.5	0.5
	8	3	0.35	1	0.5

Finally, when we applied 8 V with a settling time of 1 Ts, the signal became higher than all previous signals with a final value of 0.85 (Fig. 17).

With load = 10: In this section, the motor of the mobile robot wheels was tested under a load value of 10 at different voltages (4, 6 and 8 V) and varied settling times (Table 3).

The signal under a load value of 10 and voltage of 4 V is oscillated at the initial stage of the experiment. Then, the signal stabilized at a settling time of 0.25 Ts with a final value of 0.1 (Fig. 18).

The signal at a voltage of 6 V and a settling time of 0.53 Ts is higher than that obtained at a voltage of 4 V with a final value of 0.24 (Fig. 19).

Finally, the signal at a voltage of 8 V and a settling time of 1.5 Ts is the highest among the other signals (4 and 6 V) with a final value of 0.35 (Fig. 20).

CONCLUSION

In this study, we investigated mobile robot movement by controlling the driving motors of a two-wheeled mobile robot. We find that the motors produce a certain output angle with respect to the control signal, such that the robot can perform a curved motion at a certain speed and radius. If the angular speed of the right motor is greater than that of the left motor, then the robot will turn to the left and vice versa. However, if the steering motor outputs are equal, then the mobile robot would drive along a straight line.

Hence, the dynamics of the mobile robot is influenced by the time constants of the two-wheeled driving motors. In the case where the command for the speeds of the wheels is equal and the time constant for one command is larger than the other, the mobile robot will deviate from the preferred trajectory. The action of the controller will cause the robot to oscillate about the preferred path of motion. Finally, different time constants of the driving motors were used to simulate undesirable external disturbances.

REFERENCES

A˚ström, K.J. and P.R. Kumar, 2014. Control: A perspective. Automatica, 50(1): 3-43.

Choudhury, D.R., 2005. Modern Control Engineering. Prentice Hall, New Delhi.

Durieu, C., H. Clergeot and F. Monteil, 1989. Localization of a mobile robot with beacons taking erroneous data into account. Proceeding of the IEEE International Conference on Robotics and Automation, 2: 1062-1068.

Fukao, T., H. Nakagawa and N. Adachi, 2000. Adaptive tracking control of a nonholonomic mobile robot. IEEE T. Robotic. Autom., 16(5): 609-615.

Kanayama, Y., Y. Kimura, F. Miyazaki and T. Noguchi, 1991. A stable tracking control method for a non-holonomic mobile robot. Proceeding of the IEEE/RSJ International Workshop on Intelligent Robots and Systems '91. Intelligence for Mechanical Systems (IROS'91), 3: 1236-1241.

Le-Anh, T. and M.B.M. De Koster, 2006. A review of design and control of automated guided vehicle systems. Eur. J. Oper. Res., 171(1): 1-23.

Micaelli, A.P.M., C. Tahmi, L. Boissier and J.M. Detriche, 1989. Controle-Commande embarque pour robots mobiles. Agrotique, Bor¬deaux.

Morin, P. and C. Samson, 2008. Motion Control of Wheeled Mobile Robots. Springer Handbook of Robotics, Springer, pp: 799-826.

Papadopoulos, E. and J. Poulakakis, 2000. Trajectory planning and control for mobile manipulator systems. Proceeding of the 8th IEEE Mediterranean Conference on Control and Automation.

Ronzoni, D., R. Olmi, C. Secchi and C. Fantuzzi, 2011. AGV global localization using indistinguishable artificial landmarks. Proceeding of the IEEE International Conference on Robotics and Automation (ICRA, 2011), pp: 287-292.

Sampei, M., T. Tamura, T. Itoh and M. Nakamichi, 1991. Path tracking control of trailer-like mobile robot. Proceeding IEEE/RSJ International Workshop on Intelligent Robots and Systems' 91. Intelligence for Mechanical Systems (IROS'91), 1: 193-198.

Samson, C., 1992. Path following and time-varying feedback stabilization of a wheeled mobile robot. Proceeding of the International Conference on Control, Automation, Robotics and Vision (ICARCV).

Samson, C. and A. Micaelli, 1992. Trajectory tracking for unicycle type and two steering wheels mobile robots. Proceeding of the ICARV, pp: RO-13.1.

Sharef, S.M., W.K. Sa'id and F.S. Khoshaba, 2010. A rule-based system for trajectory planning of an indoor mobile robot. Proceeding of the 7th International Multi-Conference on Systems Signals and Devices (SSD, 2010), pp: 1-7.

Sharma, G. and J. Martin, 2009. MATLAB®: A language for parallel computing. Int. J. Parallel Prog., 37(1): 3-36.

Singh, S.J. and D.H. Shin, 1989. Position based path tracking for wheeled mobile robots. Proceeding of the IEEE-RSJ International Workshop on Intelligent Robots and Systems.

Vis, I.F.A., 2006. Survey of research in the design and control of automated guided vehicle systems. Eur. J. Oper. Res., 170(3): 677-709.

Zhang, Q., L. Lapierre and X. Xiang, 2013. Distributed control of coordinated path tracking for networked nonholonomic mobile vehicles. IEEE T. Ind. Inform., 9(1): 472-484.